Int. J. Multiphase Flow Vol. 18, No. 3, pp. 455–463, 1992
Printed in Great Britain.

0301-9322/92 $5.00 + 0.00

RIVULET MEANDERS ON A SMOOTH HYDROPHOBIC SURFACE

T. NAKAGAWA
Department of Mechanical System Engineering, Kanazawa Institute of Technology, Kanazawa, Ishikawa 921, Japan

(Received 6 June 1991; in revised form 28 December 1991)

Abstract—An experimental study of the rivulet emanating from a pipe mouth on a glassy hydrophobic surface has been performed. With increasing discharge rate, the rivulet exhibits four different patterns, viz. droplet, stable-meandering stream, unstable-meandering stream and restable stream. There exists an inherent periodicity in the restable stream, which has been attributed to the mechanism leading to the periodic water jet emanating from a rectangular nozzle.

Key Words: rivulet, hydrophobic surface, film flows

1. INTRODUCTION

A windowpane speckled with raindrops exemplifies an enigma in the physics of fluids (Walker 1985). When the rain runs down the windowpane in a stream, why does it normally meander instead of going straight? Such a stream will be, hereafter, referred to as a *rivulet* which flows on a smooth hydrophobic surface due to the gravity component along the surface (Towell & Rothfeld 1966). Rivulets are also seen on automobile windshields or on the walls of a shower. The perimeter of the contact area between the rivulet and the solid surface is called the triple-phase line. The angle at which the water touches the solid surface at the triple-phase line is called the contact angle. It is measured between the solid surface and the tangent to the water surface.

In the early part of the nineteenth century, Thomas Young (1805) stated that the contact angle for a liquid drop is determined by the tendency toward equilibrium of the three tensions pulling on the triple-phase line. However, the common observation that water drops cling to a windowpane indicates that the theory is not directly applicable. Obviously a triple-phase line is in equilibrium over a range of contact angles, and not at a single value. The liquid spreads over the surface of a solid body only when the contact angle exceeds some upper limit, while it contracts only when the contact angle drops below some lower limit. After either event the contact angle is again within the range of values that allows stability. The upper limit is called the advancing contact angle; the lower one the receding contact angle; the phenomenon is referred to as the *contact-angle hysteresis*. It is the hysteresis that enables a liquid drop to cling to an inclined surface. Why a triple-phase line displays hysteresis is a subject of current research. Dussan & Chow (1983) have analyzed a sliding drop problem and shown that contact-angle hysteresis is its most important characteristic.

Since water molecules in the rivulet are pulled downward by gravity, it may be natural to expect the locus to be straight. Yet, in many experiments (e.g. Tanner 1960; Kern 1969, 1971; Gorycki 1973; Nakagawa 1982; Sieber 1983; Nakagawa & Scott 1984; Culkin & Davis 1984; Davis & Tinker 1984), the rivulet meanders, developing bends that connect relatively straight stretches which slant to one side or the other. Furthermore, rivulets display a large variety of intriguing instability phenomena. Kern (1969, 1971), for example, describes the break-up of rivulets into drops, rivulet meandering and turbulent rivulets. It is suggested by Davis (1980) that droplet formation is due to capillary instability, where the surface tension on the liquid–air interface causes a capillary pressure gradient that enhances small interfacial corrugations. Large-amplitude surface waves on the rivulet are also apparent in many situations.

Progress of the mathematical theory on rivulet meandering is relatively slow. The existing theory is essentially limited to the straight rivulet solution (Towell & Rothfeld 1966; Allen & Biggin 1974). Towell & Rothfeld (1966) have treated a cylindrical static meniscus, straight parallel static contact lines and unidirectional steady parallel flow down a smooth solid surface. Allen & Biggin (1974)

have extended Towell & Rothfeld's zero-order solution to a first-order solution, and calculated the velocity distribution within the rivulet.

Davis (1980) has investigated capillary instabilities of a small static rivulet on a horizontal surface by linear stability theory. The triple-phase lines treated in the theory are: moving but have fixed contact angles; or moving but have contact angles which are smooth functions of contact-line speeds. No results have been obtained by Davis (1980) for a system that displays contact-angle hysteresis, because this common phenomenon is outside the realm of linear stability theory. Weiland & Davis (1981) have studied long-wave instabilities for flat rivulets on a vertical wall, incorporating the triple-phase line conditions into their analysis. Their results suggest that contact-angle hysteresis would lead to absolute stability of rivulets against small-amplitude long waves. Young & Davis (1987) have examined a three-dimensional rivulet flowing down a vertical plane, assuming a linear relationship between the speed of the contact line and the contact angle, without considering contact-angle hysteresis: kinematic-wave instabilities are predicted for wide rivulets with immobile contact lines, while capillary break-up is predicted for narrower rivulets with mobile contact lines. The expression for the growth rate depends weakly on the slip between the liquid and solid near the contact line, but strongly on the shape of the rivulet and the mobility of the contact lines.

The main purpose of this study is to elucidate how the rivulet varies in shape and behaviour in relation to the discharge rate and slope. The present study covers discharges up to 20 cm^3/s, which is over five times greater than those in Nakagawa & Scott's (1984) previous study.

2. EXPERIMENT

Figure 1 shows a schematic diagram of the experimental arrangement. The glassy smooth Plexiglas plate showing no waves or any other surface irregularities was 100 cm long and 60 cm wide, and the water tank allowed a constant discharge through a vinyl pipe of 8 mm dia. The pipe mouth was arranged on the centerline of the plate, at a point 20 cm down the slope from the upper edge. The experimental variables were the discharge rate Q, measured by weighing the water discharged in a given time, and the surface slope α, measured with a protractor. As the experiments progressed, it was realized that the rivulet on the surface was restabilized once the discharge exceeded an upper limit. Therefore, the maximum discharge for each surface slope was chosen as the amount above which the rivulet becomes stable again. The surface slope was set at 2° initially and then was varied from 5° to 80°, at 5° intervals.

The cross section of the rivulet was measured pointwise, using a slender needle of 0.1 mm dia, held perpendicular to the plate surface. Height measurements were made at 5 mm intervals along

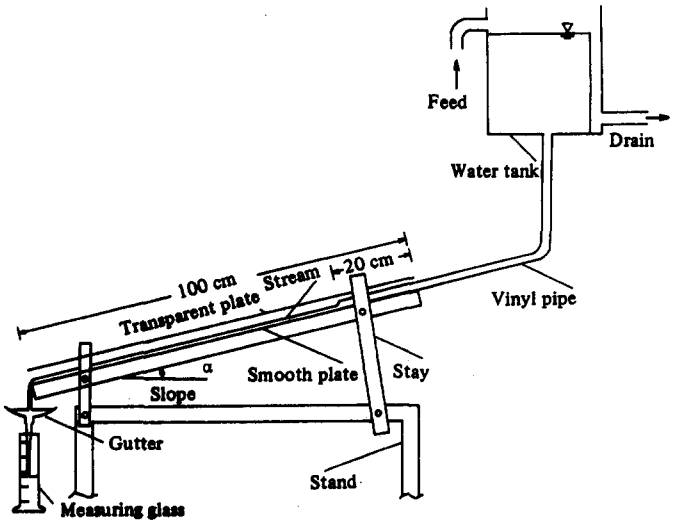

Figure 1. Schematic diagram of the experimental arrangement.

the direction of maximum slope, and at 1 mm intervals along a line normal to the central axis of the rivulet. The contact angle is determined from the angle of the measured cross-sectional shape of the rivulet at the contact lines. The sinuosity (ratio of the total rivulet length to the projection of the rivulet on the line of maximum slope of the surface) is determined as follows: the total rivulet length of the stable-meandering stream was determined by tracing the plane locus of the central axis, using ink onto the transparent plate. When the meandering stream is unstable, only the stable portion of the rivulet is considered for determination of the sinuosity; this stable portion represents well the entire rivulet. The motion of the rivulet is very sensitive to the condition of the plate surface. For example, the rivulet locus tends to follow the wetted parts. Thus, the surface was carefully dried for each experimental run, wiping it with soft hygroscopic tissues, and then waiting for about 30 min before the next run.

3. RESULT

The first two patterns, *viz.* droplet and stable-meandering stream, have been well-documented in the existing literature (e.g. Kern 1969, 1971; Nakagawa & Scott 1984), so in this section only results for the last two patterns, *viz.* unstable-meandering stream and restable stream, will be presented.

Figure 2 shows an unstable-meandering stream on the surface at a discharge rate $Q = 4.70\ \text{cm}^3/\text{s}$ and for a surface slope $\alpha = 10°$. The locus of the downstream portion varies with time, but the upstream portion appears not to move. A number of water droplets and child-rivulets left on the surface of the Plexiglas plate were produced by the unsteady motion of the mother-rivulet. It may be worth noting here that the child-rivulets located on the right of the mother-rivulet also meander. Thus, it may be natural to consider that the origin of the rivulet meandering is in the stream itself, and not in possible fluctuations due to the flow discontinuity at the pipe mouth or turbulence in the pipe.

Figure 3 shows another unstable-meandering stream on the surface at a discharge rate $Q = 14.28\ \text{cm}^3/\text{s}$ and a surface slope $\alpha = 10°$. In this figure, a number of characteristic features of the stream can be noted: following the pipe mouth, the rivulet width follows an increase/decrease cycle several times and then the rivulet delineates an unstable but sinuous locus, having an almost constant width.

Figure 4 shows a restable stream on the surface at a discharge rate $Q = 23.30\ \text{cm}^3/\text{s}$ and a surface slope $\alpha = 10°$. It is this novel rivulet pattern that was observed when the discharge rate was suddenly increased to a large value. It can be noted that the local maximum width of the rivulet at each antinode decreases with increasing distance from the pipe mouth, while the local minimum width at each node increases. The number of increase/decrease cycles of the rivulet width are greater than those in figure 3, and the rivulet becomes straight downstream.

Figure 5 illustrates how the sinuosity of the meandering stream S depends on the discharge rate Q, where parameter α is the surface slope. This figure indicates that irrespective of the surface slope, as long as the discharge rate is small, the sinuosity is approx. 1.0, but increases with increasing discharge rate and reaches a peak value once. Then, the sinuosity decreases with increasing discharge rate, and approaches a constant value of about 1.0. Note that the discharge rate at which the sinuosity reaches its peak value also depends on the surface slope. The peak value of the sinuosity first increases with the slope and reaches a maximum at $\alpha = 20°$. After this maximum, the peak value of the sinuosity fluctuates with the slope, but on average decreases gradually with increasing surface slope.

Figure 6 illustrates that the rivulet on the smooth surface exhibits four different patterns, *viz.* droplet, stable-meandering stream, unstable-meandering stream and restable stream. It is, therefore, clear that the rivulet experiences three transitions as the discharge rate is increased. The first transition occurs once the discharge rate reaches a value sufficient to maintain continuous flow on the surface. Immediately after the first transition the sinuosity is approx. 1.0. The second transition occurs just before the sinuosity reached its peak value; and the third transition will take place when the rivulet is restabilized. The sinuosity of the unstable-meandering stream decreases with increasing discharge. However, after the rivulet is restabilized, the sinuosity becomes about 1.0 again.

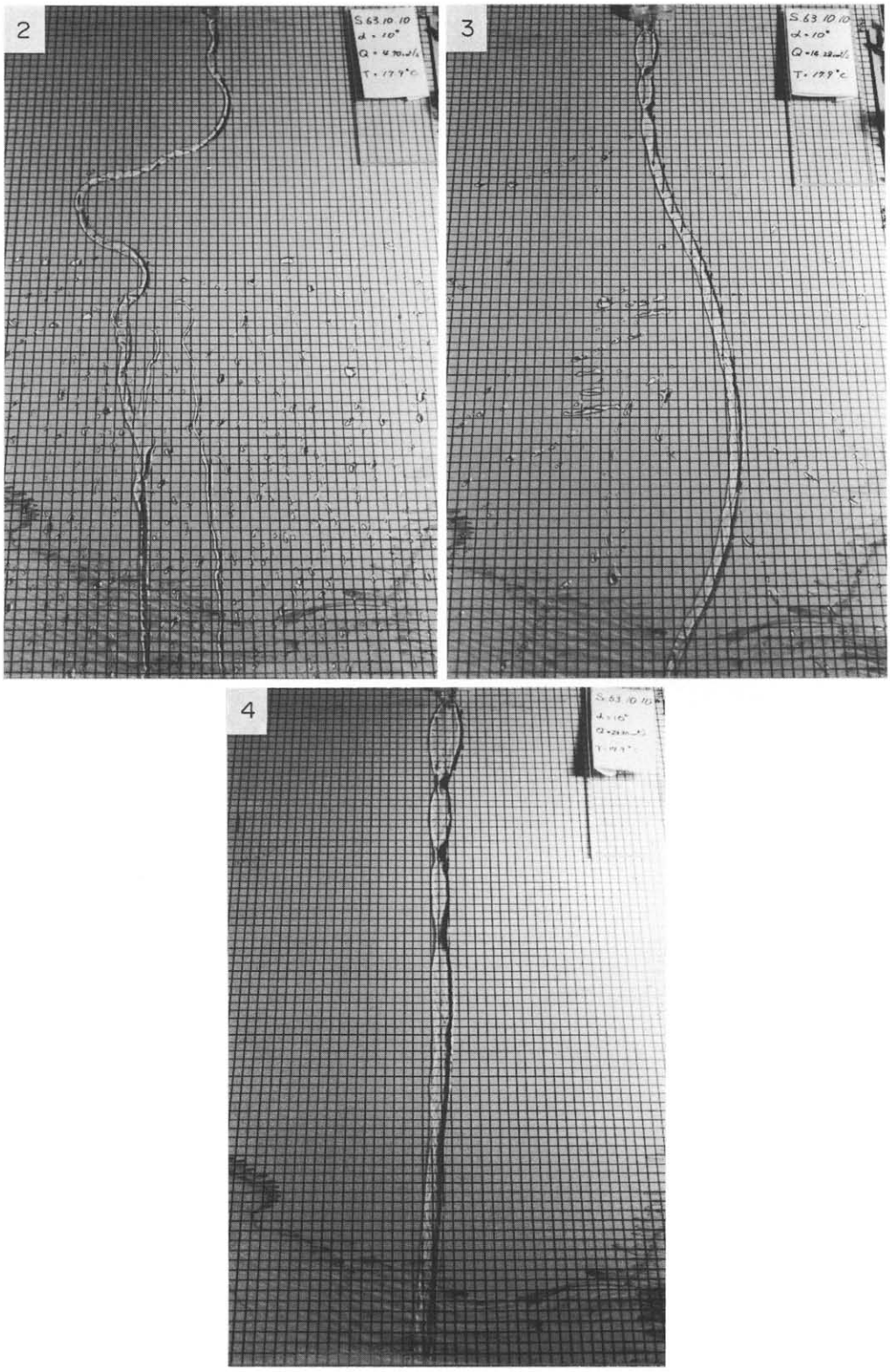

Figure 2. Unstable-meandering stream on the smooth hydrophobic Plexiglas surface. $Q = 4.70\,\text{cm}^3/\text{s}$, $\alpha = 10°$.

Figure 3. Unstable-meandering stream on the smooth hydrophobic Plexiglas surface. $Q = 14.28\,\text{cm}^3/\text{s}$, $\alpha = 10°$.

Figure 4. Restable stream on the smooth hydrophobic Plexiglas surface. $Q = 23.30\,\text{cm}^3/\text{s}$, $\alpha = 10°$.

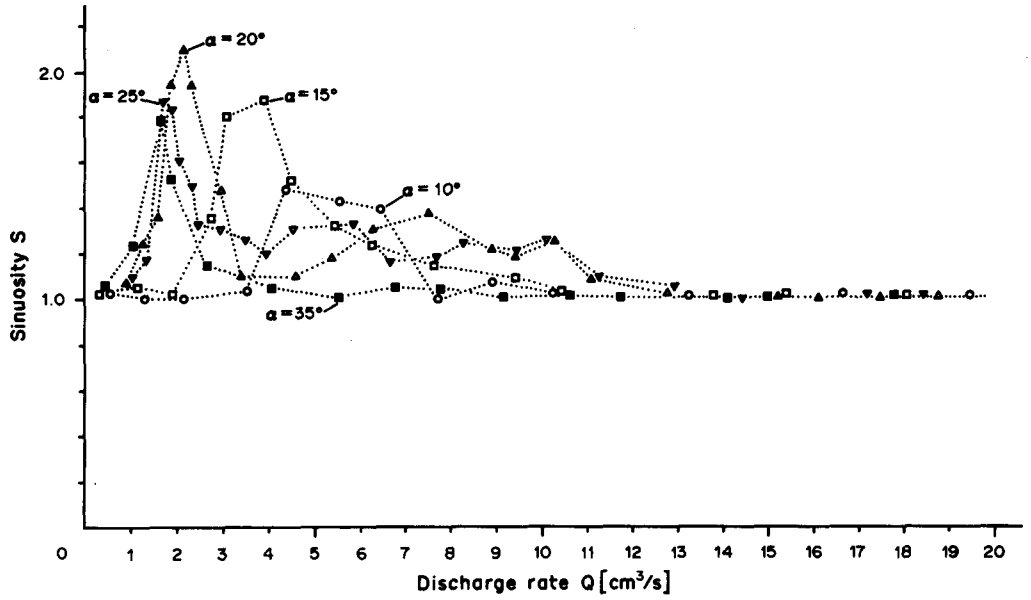

Figure 5. Sinuosity of the rivulet S against discharge rate Q for each surface slope α.

The first three rivulet patterns have been already identified by Kern (1969, 1971) and Nakagawa & Scott (1984), but the fourth rivulet pattern has been observed for the first time during the present experiment. The first transition depends weakly on the surface slope and occurs at values of the discharge rate ranging from 0.10 to 0.15 cm^3/s. The second transition depends on the surface slope as well as on the discharge rate: until the slope becomes about 40°, the second critical discharge rate decreases from ~ 3.5 to ~ 0.8 cm^3/s with increasing slope. However, once $\alpha > 40°$, this critical discharge rate becomes almost independent of the slope. The third transition also depends on the surface slope as well as on the discharge rate: it takes place at $Q \simeq 12$ cm^3/s for $\alpha = 5°$ and increases with increasing slope, taking the maximum value of $Q \simeq 19.5$ cm^3/s for $\alpha = 70°$. However, this critical discharge rate decreases suddenly with a further increase in the surface slope and takes the value of $Q \simeq 11$ cm^3/s for $\alpha = 80°$. It may be noteworthy that the third critical discharge rate increases rapidly between $\alpha \simeq 20°$ and 40°.

It is observed that once the discharge rate exceeds the third critical value, the locus of the rivulet axis on the smooth hydrophobic Plexiglas surface becomes straight again: at the pipe mouth, the rivulet expands abruptly both to the left and right, whereas the expansion in the direction normal to the surface is restricted by gravity acting on the rivulet. It is clear that the excess discharge makes the contact area between the rivulet and the surface large. Therefore, even if the left (or right) contact angle became greater than the right (or left) contact angle to such a degree that rivulets having a smaller discharge rate than the third critical value would have moved, it may not be possible for the rivulet having a greater discharge rate than the third critical value to change its locus.

Figure 7 shows the plane view of a restable stream emanating from the pipe mouth, and the measured cross sections at 10 mm intervals along the direction of maximum surface slope at a discharge rate $Q = 22.80$ cm^3/s and a surface slope $\alpha = 10°$. Figure 8 shows how the cross-sectional area A of the rivulet and the width w vary, depending on the distance x from the pipe mouth. The width w increases with increasing distance and takes the maximum value at $x = 7$ cm. Then, the width decreases from $x = 7$ to 17 cm, at which point it takes a local minimum value. Then, the width increases again with distance. In absolute values, the rate of decrease of the width with distance from $x = 7$ to 17 cm is smaller than the rate of increase with distance from the pipe mouth to $x = 7$ cm. Moreover, the rate of increase of the width with distance downstream from $x = 17$ cm is slightly smaller than the rate of decrease rate from $x = 7$ to 17 cm. The increase/decrease cycle of the rivulet width is repeated several times along the locus, and then the rivulet is transformed into a smooth one, having an almost constant width, as shown in figures 3 and 4. Note that cross

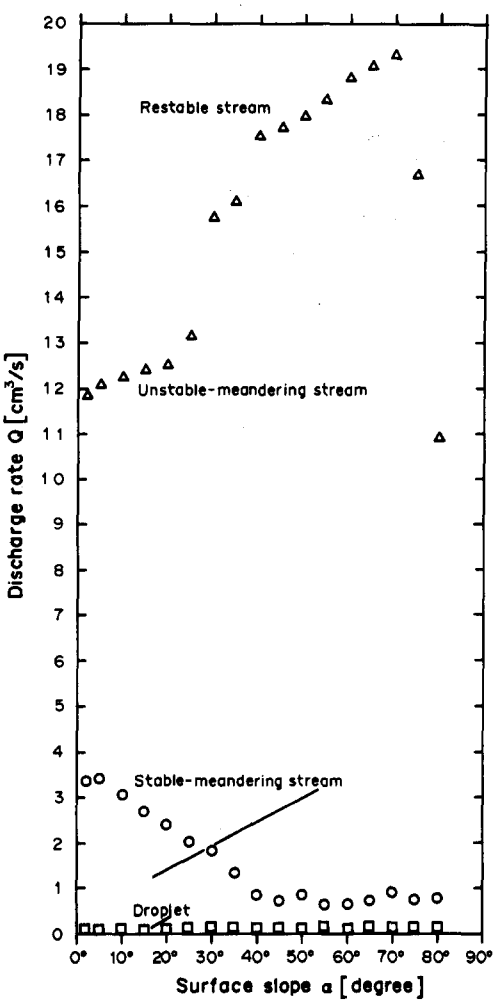

Figure 6. Four rivulet patterns on the smooth hydrophobic Plexiglas surface demarcated on the α–Q plane.

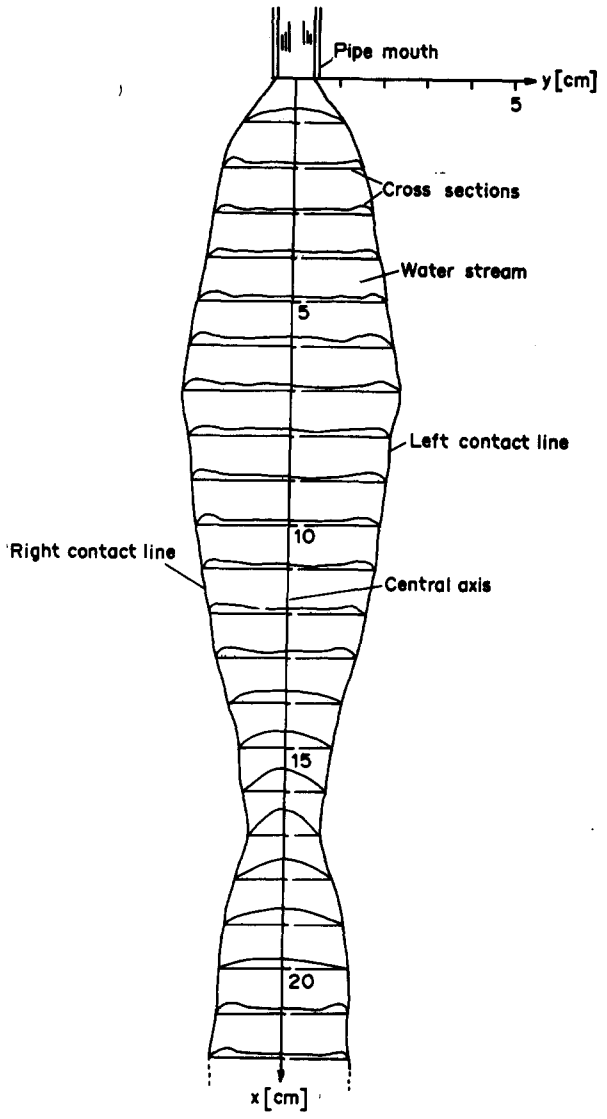

Figure 7. Plane form of a restable stream and its cross sections at 10 mm intervals along the direction of maximum slope. $Q = 22.80\,\text{cm}^3/\text{s}$, $\alpha = 10°$, $S = 1.0$.

sections around each node have a single peak near the central axis, while the rest of the cross sections have double peaks near the edges.

After expansion at the pipe mouth, the cross-sectional area decreases up to $x \simeq 2$ cm, and has several minima and maxima, as shown in figure 8. The rate of decrease of the cross-sectional area with distance from $x = 6$ to 11 cm is smaller than the rate of increase with distance from $x = 2$ to 6 cm. Moreover, the rate of increase of cross-sectional area from $x = 11$ to 18 cm is smaller than the rate of decrease from $x = 6$ to 11 cm. It is interesting to note in figure 8 that the extrema of the cross-sectional area of the rivulet do not coincide with those of the rivulet width in general. The cross-sectional area reaches a local maximum not only near the antinode of the rivulet width, but also near the node. The reason for this will be discussed in the next section.

Figure 7 shows the contact-angle hysteresis very clearly: it is found that both the left and right contact lines do not move for a range of contact angles between 10° and 71°. It may be worth pointing out here that Culkin & Davis (1984) have found that the advancing and receding contact angles for a water drop placed on a Plexiglas plate were 74° and 47°, respectively. It is suggested that the difference in the range of contact angles is caused by the nature of the force balance: in

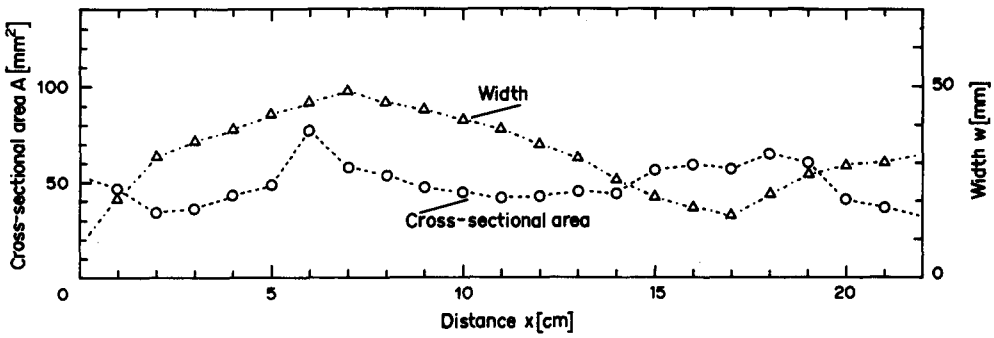

Figure 8. Variation of the cross-sectional area A and of the rivulet width w with distance x along the direction of maximum slope.

the case of rivulets the contact angles are determined by a *dynamic* force balance; and in the case of drops, by a *static* force balance.

4. DISCUSSION

Variation of the cross-sections of the restable stream downstream from the mouth of the pipe suggests the existence of an inherent periodicity in the rivulet. The origin of this periodicity will be discussed below.

When water exits from the pipe mouth and contacts the smooth surface, the rivulet formed experiences a strong expansion to both the right and left. This phenomenon has similarities with a water jet emanating from a rectangular nozzle and falling vertically downwards (e.g. Rayleigh 1879; Nakagawa & Nakagawa 1992). In the latter case a water sheet having a rectangular cross section is formed at the nozzle exit, then contracts towards the central axis to minimize its surface area and finds a minimum value at some distance from the nozzle. However, near the point of minimum width, the contraction overshoots and the water expands in the direction normal to that of the original sheet; the width of the water sheet increases with increasing distance from the point of minimum width, and takes a maximum value at a point downstream. Following the point of maximum width, the width of the water sheet decreases again. It seems natural to consider that the surface tension takes the role of the restoring force in this periodic motion.

It is suggested here that the periodic flow pattern depicted in figure 7 is induced essentially by the same mechanism as that in a water jet emanating from a rectangular nozzle: figure 8 shows that the cross-sectional area of the rivulet decreases up to $x = 2$ cm from the pipe mouth, and then increase from $x = 2$ to 6 cm. The discharge rate is kept at a constant value, so that the points of each maximum rivulet cross-section correspond to local minimum velocities (or maximum pressures) and vice versa: the pressure in the rivulet decreases from the pipe mouth to $x = 2$ cm, and then increases from $x = 2$ to 6 cm, at which the cross-sectional area and/or surface area of the rivulet per unit longitudinal distance take a local maximum value. Downstream from the local maximum cross-sectional area, the rivulet is contracted by the surface tension, and the cross-sectional area decreases from $x = 6$ to 11 cm. In this range the pressure decreases, and the flow in the rivulet is accelerated. However, similarly to a water jet emanating from a rectangular nozzle, there is an overshoot in the contraction of the rivulet, and this results in an expansion in the direction normal to the plate. Indeed, the height of the cross section near the central axis increases gradually from $x = 11$ to 18 cm, as can be noted in figure 7. Contraction of the rivulet starts again at $x = 18$ cm, at which point the cross-sectional area takes another local maximum value, although the direction of the contraction is now normal to the plate.

The oscillatory motion leading to the present periodic flow pattern may, however, be retarded by the viscous effects, either at the contact area between the surface and the rivulet and/or the area between the surrounding air and the rivulet. Thus, the actual number of expansion–contraction processes of the rivulet must depend on the degree of the initial expansion at the pipe mouth and the degree of the subsequent viscous dissipation. These fascinating questions could be clarified by

examining the effects of pipe diameter, discharge rate, slope and fluid properties, but they are beyond the scope of the present study.

5. CONCLUSION

It is found that with increasing discharge rate, the rivulet exhibits four different patterns, *viz.* droplet, stable-meandering stream, unstable-meandering stream and restable stream. The first three patterns have been observed but the fourth pattern has been identified for the first time in the present study.

The first transition from droplet to stable-meandering stream occurs once the discharge rate reaches a value sufficient to maintain continuous flow on the surface. Thus, immediately after the first transition the sinuosity is approx. 1.0. The second transition from the stable-meandering to unstable-meandering stream occurs just before the sinuosity reaches its peak value. The sinuosity increases rapidly just before this peak value. The third transition from the unstable-meandering to restable stream is completed when the rivulet is restabilized. During the third transition, the sinuosity decreases with increasing discharge rate. The central axis of the restable stream is almost straight, and thus the sinuosity becomes again approx. 1.0.

Once the rivulet is restabilized, its plane form becomes almost symmetrical with respect to the central axis. In the case of the restable stream, after exiting from the pipe an increase/decrease cycle of the rivulet width is repeated several times, but the rivulet trajectory is gradually transformed into a smooth one, and its width becomes almost constant. During the increase/decrease cycle, cross sections of the restable stream near each node have a single central peak while the rest of the cross sections have double peaks at the edges.

It is suggested that there exists an inherent periodicity in the restable stream, and that this periodicity can be attributed to the same mechanism as a water jet emanating from a rectangular nozzle.

Acknowledgements—The author is grateful to Professor G. Yadigaroglu (ETH Zürich) and the anonymous referees for their critical comments on the original manuscript of this paper which contributed to the present quality.

REFERENCES

ALLEN, R. F. & BIGGIN, C. M. 1974 Longitudinal flow of a lenticular liquid filament down an inclined plane. *Phys. Fluids* **17,** 287–291.

CULKIN, J. B. & DAVIS, S. H. 1984 Meandering of water rivulets. *AIChE Jl* **30,** 263–267.

DAVIS, S. H. 1980 Moving contact lines and rivulet instabilities. Part 1: the static rivulet. *J. Fluid Mech.* **98,** 225–242.

DAVIS, T. R. H. & TINKER, C. C. 1984 Fundamental characteristics of stream meanders. *Bull. Geol. Soc. Am.* **95,** 505–512.

DUSSAN, V. E. B. & CHOW, R. T.-P. 1983 On the ability of drops or bubbles to stick to non-horizontal surfaces of solids. *J. Fluid Mech.* **137,** 1–29.

GORYCKI, M. A. 1973 Hydraulic drag: a meandering initiating mechanism. *Bull. Geol. Soc. Am.* **84,** 175–196.

KERN, J. 1969 Zur hydrodynamik der rinnsale. *Verfahrenstechnik* **3,** 425–430.

KERN, J. 1971 Stabilitätsprobleme der Rinnalströmung. *Verfahrenstechnik* **5,** 289–294.

RAYLEIGH, LORD 1879 On the capillary phenomena of jets. *Proc. R. Soc. Lond.* **A24,** 71–97.

NAKAGAWA, T. 1982 On the role of discharge in sinuosity of stream on a small plate. *Naturwissenschaften* **69,** 142–143.

NAKAGAWA, T. & SCOTT, J. C. 1984 Stream meanders on a smooth hydrophobic surface. *J. Fluid Mech.* **149,** 89–99.

NAKAGAWA, T. & NAKAGAWA, R. JR 1992 A novel oscillation phenomenon of the water rivulet on a smooth hydrophobic surface. *J. Fluid Mech.* Submitted.

SIEBER, M. 1983 *Experimentelle Untersuchungen zum Rinnsalmäander*, Bericht 5. Max-Planck-Institut für Strömungsforschung, Göttingen. In German.

TANNER, W. F. 1960 Helicoidal flow, a possible cause of meandering. *J. Geophys. Res.* **65,** 993–995.

TOWELL, G. D. & ROTHFELD, L. B. 1966 Hydrodynamics of rivulet flow. *AIChE Jl* **12,** 972–980.

WALKER, J. 1985 What forces shape the behaviour of water as a drop meanders down a windowpane? *Scient. Am.* **253,** 132–137.

WEILAND, R. H. & DAVIS, S. H. 1981 Moving contact lines and rivulet instabilities. Part 2: long waves on flat rivulets. *J. Fluid Mech.* **107,** 261–280.

YOUNG, G. W. & DAVIS, S. H. 1987 Rivulet instabilities. *J. Fluid Mech.* **176,** 1–31.

YOUNG, T. 1805 An essay on the cohesion of fluids. *Phil. Trans. R. Soc. Lond.* **95,** 65–87.